

RESEARCH

Open Access



Imaging of sino-nasal inverted papilloma: How can we emphasize the usefulness of the “striated pattern” sign?

Mohamed Eid and Lamya Eissa*

Abstract

Background: Inverted papilloma (IP) is an uncommon sino-nasal neoplasm with potentially distinctive MRI and CT features. The MR “striated” imaging pattern has been reported as a valuable MR imaging feature of IP. The purpose of this study was to validate the usefulness of this sign using detailed criteria of the sign itself.

Results: All imaging findings were described for 16 patients in descriptive pattern. The nasal involvement showed highest prevalence followed by the maxillary sinus. The bony changes include remodeling and defects ($n = 6$), remodeling only ($n = 4$), and None ($n = 6$). Changes were severe 1/10, moderate in 3/10, and mild 5/10. Focal hyperostosis was seen in six. A striated pattern was “diffuse” in all 16 (100%) of the IPs; it followed a *certain direction* in all 16 patients: divergent ($n = 6$), convoluted ($n = 2$), and parallel ($n = 8$). Divergent growth from focal hyperostosis was seen ($n = 4$). Visibility of the sign was superior in T2 images ($n = 11$), superior in enhanced images ($n = 3$), and equal in both ($n = 2$).

Conclusions: The striated pattern is a reliable MR imaging feature of sino-nasal IPs. Validity and usefulness of this sign can be emphasized by defining parameters of the signs itself including the following: diffusivity, direction of striations and relation to hyperostosis, and comparing visibility in both T2 and GAD-enhanced images, as well as combining this imaging signature with remodeling bony changes < 1.5 .

Keywords: CT, MRI, Inverted papilloma, Sino-nasal, Maxillary

Background

Inverted papillomas (IPs), though being an uncommon benign epithelial neoplasm, have generated considerable interest through literature. This interest is that though they are benign, they are locally aggressive and have a propensity to recur, and are sometimes associated with malignancy [1, 2]. Recurrent disease and metachronous carcinoma can even develop after a prolonged period of time. The term *papilloma* means neoplasia with epithelial growth, while the US National Cancer Institute’s had defined inverting papilloma as a type of tumor in which surface epithelial cells grow downward into the underlying connective tissue, and thus have been coined the term (inverting = inverted) [3].

Pre-operative imaging of the sinuses is essential before a treatment plan can be proposed to provide additional information for staging and treatment planning of sino-nasal masses including the inverted papillomas [4–6]. Both CT and MRI are typically performed for evaluation of sinus tumors and they are complementary modalities in evaluating disease extent, and in distinguishing tumor from infection, retained secretions, and granulation or scar tissue; all are better resolved by MRI [4–6].

Though imaging cannot differentiate the sino-nasal tumors, Ojiri et al. [7] discussed some potentially distinctive features of inverted papilloma on MR imaging, of which a convoluted cribriform pattern on T2 and enhanced T1-weighted images may be distinctive in 80% of cases. This sign, the convoluted cerebriiform pattern (CCP), can be displayed on MR imaging by the characteristic alternating hypointense and hyperintense bands on T2-weighted and contrast-

* Correspondence: lamya.eissa@gmail.com

Alexandria Faculty of Medicine, Radiology Department, Alexandria, Egypt

enhanced T1-weighted images, reflecting underlying histopathology of the lesion. This was further studied and discussed by Branes et al. [8], Maroldi et al. [9], and Jeon et al. [10].

The purpose of this retrospective study was to evaluate the same sign, the CCP, as depicted in the MRI of proven 16 cases to reveal some imaging details of the same sign which could elucidate and highlight the specificity of this imaging signature in making definite pre-operative diagnosis of inverted papilloma.

Methods

Patients

The protocol of our retrospective study had approval made by the Institutional Review Board (IRB) of our university hospital. Patient approval or informed consent was not required for the review of images and clinical records. Of all patients referred to our institution between January 2018 and January 2019, sino-nasal inverted papillomas were confirmed in pathological specimens after surgery in 25 patients. Only 16 out of 25 patients with pre-operative imaging findings of striated pattern and had both CT and MRI made for pre-operative evaluation. Patients who had other variegated non-striated imaging appearance, as well as those who had single imaging exam, either only CT or MRI had been excluded. The CT and MRI images obtained in these patients were retrospectively reviewed.

Imaging techniques

The MRI examination studies were made on *one closed* 1.5 Tesla Magnet (Siemens; Avanto, Germany). A dedicated multi-channel head and neck coil was used in all patients. MRI exam included the following sequences: axial T1 turbo spin echo (TSE), axial T2 turbo spin echo with and without fat suppression, and axial and coronal T2 sequence without fat suppression. The scanning parameters were as follows: a slice thickness of 5 mm was used with an inter-slice gap of 3 mm, and a 16 × 16 cm field of view (FOV), with 5 averages used. T1-weighted images (TR, 550 ms; TE, 10 ms; 256 × 256 matrix) and turbo spin echo T2-weighted images (TR, 4400 ms; TE, 105 ms; 250 × 250 matrix) were used. Diffusion-weighted imaging was obtained using single-shot spin echo planar imaging in axial plane, with fat suppression made by chemical shift selective fat suppression. Diffusion was obtained by “high” repetition time (TR) of 1700 ms, “short” echo time (TE) of 100 ms, slice numbers = 30, slice thickness = 5 mm, inter-slice gap, and number of averages = 5. Three b-factors are obtained including 0, 500, and 1000 s/

mm² in the axial plane. Contrast-enhanced MRI sequence was made by manual injection of Gadolinium (GAD, Gadopentetate Dimeglumine with a dose of 0.1 mmol/kg) followed by 20 ml saline flush. Enhanced images are obtained through the lesion in axial plane and at different time intervals. Enhanced images are then obtained in three orthogonal planes with fat suppression. For CT imaging, non-contrast scans were performed on 128 and 160 multi-slice scanners (Aquillion Toshiba, Canon; Japan). Spiral scanning was performed at 120 kVp and 70 mAs. CTA was made on the same machine with parameters of 120 kV and 100 mAs. The reconstructed axial images were sent to an offline workstation (Vetria 2.2 workstation), where multi-planar reformations have been viewed including the coronal and sagittal planes.

Image analysis on MRI

All of the MR images were retrospectively reviewed by two dedicated senior and junior head-and-neck neuroradiologists who have been practicing in the field for 23 years and 12 years, respectively. The following imaging details are analyzed:

- (a) Laterality of the lesion: either *right* or *left* side. For a lesion involving a single moiety sphenoid sinus, a *midline* location is coined. *Bilateral disease* is coined only if a lesion is certainly crossing through a solid midline structure (e.g., nasal septum). So a nasal lesion crossing midline choana is not bilateral. For definitely bilateral lesion, predominance of a side is reported.
- (b) *Exact location of the lesion*: either sinus (maxillary, ethmoidal, etc.) or a nasal cavity. For a lesion occupying more than one region, a description is made by combining the two locations, e.g., naso-ethmoidal. The first component of the complex name indicates the epicenter of the lesion.
- (c) The size of the mass. This is reported in MRI because it nicely separates the outlines of the solid mass from the signal of obstructed retained sections. The *longest diameter* of the solid mass is measured in the three orthogonal planes and the longest one is the one reported in any of the three orthogonal planes in contrast-enhanced images. This is reported in centimeters (cm).
- (d) *Morphology of the lesion*. *The following have been reviewed*: *Margins* are reported only if the mass is surrounded at some portion of its surface by secretions. If the mass is all around surrounded and

in direct contact with bony sino-nasal wall, the comment on borders would be non-applicable. *T1 signal intensity*—this is reported in comparison with muscles (of mastication). T1 signal pattern is reported as “striated” or “None”. *T2 signal intensity*—this is reported as compared to visualized brain parenchyma in fat suppressed T2 images. This is reported as “iso” or “hypo” or “hypo to iso”. Also, T2 signal pattern is reported as “striated” or “None”. The pattern of striations is examined in both axial and coronal images.

For ADC values, a region of interest (ROI) will be drawn on the lesion, being sufficiently drawn at the solid portion of the lesion excluding areas of necrosis or hemorrhages. ADV value is then reported. The enhancement is reported in enhanced T1 images and reported to be either “striated” or “None”. Presence or absence of internal cysts are examined and detected first in T2 images and expected to show fluid signal comparable to sinus sections and CSF signal. The enhancement of the cysts is then examined in GAD-enhanced images (either “enhanced” or “NOT”).

CT imaging evaluation and analysis

For bony changes related to the margin of the sino-nasal inverted papilloma at sino-nasal walls, after visualizing the contour of the lesion in T2 and enhanced MRI images, the bony changes are examined in CT in direct contact with the main mass. The following have been analyzed:

- (a) The changes are reported as either “Remodeling” which means smooth expansion and compression on bone, versus “Permeative” which means aggressive pattern of destruction. If no bony changes are noted, this is reported as “None”.
- (b) The sinus or nasal walls involved are enumerated.
- (c) The extent of bony disease for remodeling without defects is reported for its length at maximum point of pressure. These are classified as mild if < 1 cm, moderate if 1–2 cm, and extensive if > 2 cm.
- (d) Presence of full thickness defect is reported and the largest defect is measured.
- (e) Presence of *calcification* within the lesion is reported.
- (f) Bony changes and extension through a bony sino-nasal drainage channel is reported. These include the OMU (Ostio-meatal unit), the sphenothmoidal recess, the fronto-ethmoidal recess. The presence or absence of *focal hyperostosis/sclerosis* is reported if it is seen in direct contact

with a solid portion of the tumor. This is considered when finding a “cone-shaped” or “plaque-like” focal bony thickening, even if this is the thickening of bony struts, like wall of the turbinate.

The changes involving a drainage channel are reported separately from the sino-nasal wall. The changes of sino-nasal walls are applicable to all walls except for the ethmoidal walls since these thin walls could be rarefied by effect of simple chronic inflammation and cannot be evaluated for certain change

The detailed evaluation of striated pattern in both coronal and axial T2- and T1-enhanced images include diffuse versus non-diffuse; diffuse is considered only if striated pattern covers more than 90% of the longest diameter. Then direction is documented as parallel, *divergent*, *convoluted*, or other. Then this sign is evaluated in relation to *focal sclerosis*, if present. Finally, visibility of the sign is compared in T2 versus contrast-enhanced images. The “diffusivity” of the “striated pattern sign” is not interrupted by smooth small intra-tumoral retention cysts.

Results

The study included 16 patients (9 males, 7 females; with age range from 29 to 85 years with mean age of nearly 57 years). Only two cases ($n = 2$) had recurrent disease and the remaining 14 cases were primary presentation. The predominant clinical complaint among patients was nasal obstruction, reported in 10 patients, all presenting primarily (Figs. 1, 2, 3, and 4). The two recurrent cases had no specific complaints and only came for routine surveillance. Two cases had epistaxis as the initial presentation, while a case was asymptomatic with incidental finding of sino-nasal mass detected in MRI exam of brain.

For the *size and location preference*, the lesion sizes ranged from 1.7 to 10.5 cm (mean, 6.2 cm), and the shape was lobulated in most of the patients ($n = 10$), smoothly oval in a single case ($n = 1$) and elongated in 4 cases ($n = 1$), while it was non-applicable in a single case filling the sinus cavity and not surrounded by secretions, so lesion margins could not be evaluated. *Unilateral* disease was predominant on the right side ($n = 7$) and on the left side ($n = 4$). Midline disease was reported in three cases ($n = 3$) with single-moiety sphenoid sinus disease (refer to Table 1).

Only two cases ($n = 2$) had bilateral disease, both had nasal disease. The *nasal* involvement had the

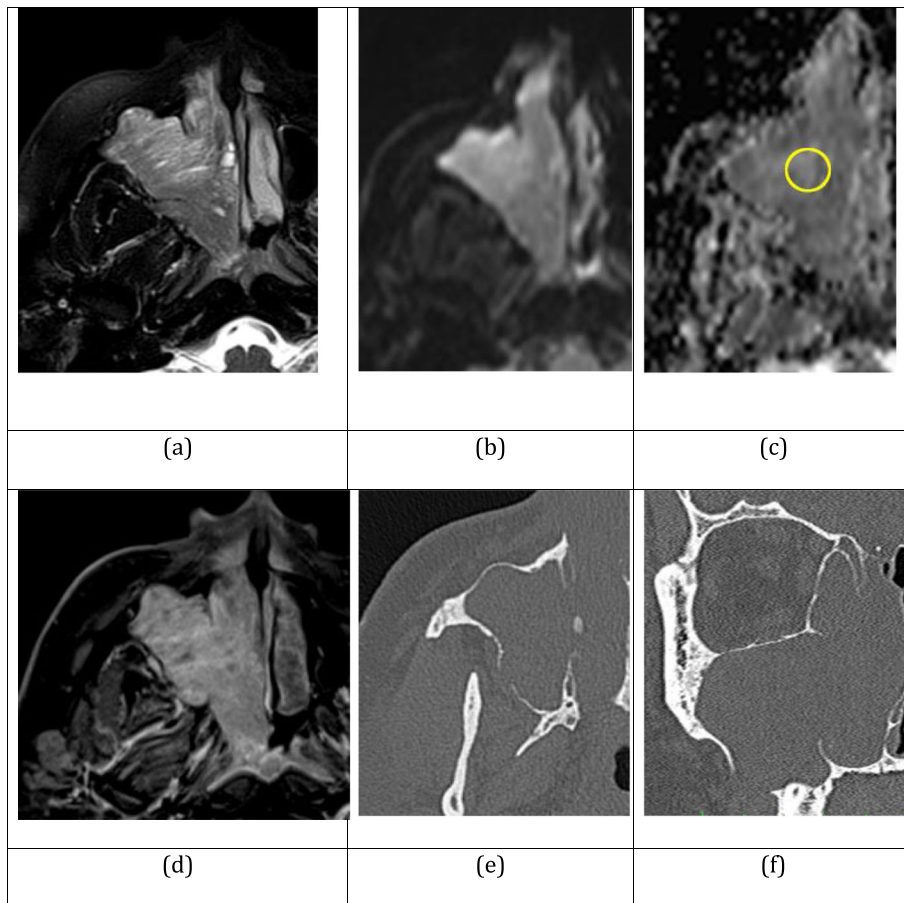


Fig. 1 A 39-year-old male with unilateral nasal obstruction and inverted papilloma. Axial T2 fat suppression (a) shows striations to good resolution better than post-gadolinium-enhanced images in (d). Axial diffusion and apparent diffusion co-efficient maps (b) and (c) showed variable apparent diffusion co-efficient values of $1.2\text{--}1.7 \times 10^{-3} \text{ cm}^2/\text{s}$. Axial computed tomography reveals smooth bony remodeling with mild scalloped smooth defect of resorption of postero-lateral wall of the maxillary sinus. Coronal computed tomography image shows marked expansion and bony rarefaction of the sinus walls including the walls at ostio-meatal unit, which is markedly, widened admitting gross nasal extension of the mass (f)

highest prevalence, being noted in ten cases ($n = 10$), with different combination of nasal and sinus involvement in eight patients and only *two strictly unilateral* nasal disease; one is showing a nasal mass between the inferior and middle turbinates and another one is epicentered at the classic site of lateral nasal wall, seen opposite the middle meatus. A case of bilateral bi-nasal disease had predominant large nasal lesions with limited frontal sinus extension. Two cases had combined maxillary sinus and nasal disease. Three cases ($n = 3$) had nasal and ethmoidal involvement with limited frontal sinus extension in two of them and maxillary extension in one. Two cases ($n = 2$) had combined nasal and maxillary sinus involvement. Three cases ($n = 3$) had isolated maxillary sinus involvement. Two patients had sphenoid-ethmoidal sinus involvement.

Regarding *bony changes* reported on CT, no definite bony changes could be noted at any sinus wall in six cases ($n = 6$); these cases showed a lesion nearly conforming to the configuration of the sino-nasal cavity. Four patients ($n = 4$) had “remodeling only” changes at sino-nasal walls. The affected walls are detailed in Table 2. Six cases ($n = 6$) had remodeling associated with smooth defects, apparently created by pressure erosion and geographic pattern of bony destruction. Only a single case had permeative destruction noted at the nasal septum with trans-septal crossing; a case proven to have squamous cell carcinoma on top of papilloma. The same patient had defects created by remodeling only. The four patients with “only remodeling” showed *limited bony changes* $< 1 \text{ cm}$. The six cases with “remodeling and defects” showed a single patient with marked extent

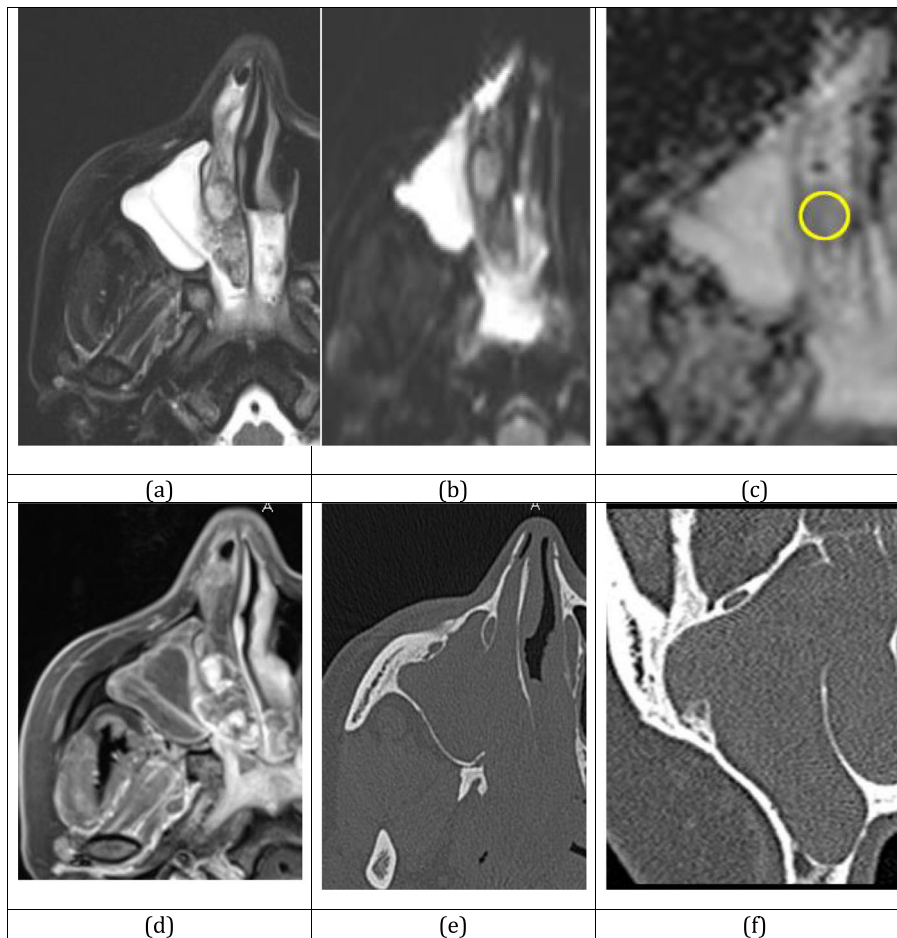


Fig. 2 A 45-year-old woman with unilateral nasal obstruction and proven nasal inverted papilloma. Axial T2-weighted fat suppression image **(a)** reveals convoluted type of striated pattern. A cystic lesion is seen not considered to interrupt the imaging signature and likely corresponds to histopathology finding of mucus retention cyst lined by glandular epithelium of the tumor. Axial diffusion and apparent diffusion co-efficient maps in **(b)** and **(c)**, respectively, show average apparent diffusion co-efficient values of $1.5 \times 10^{-3} \text{ cm}^2/\text{s}$. Axial post-gadolinium-enhanced exam reveals nodular pattern of enhancement corresponding to enhanced glands of the retention cysts. Axial computed tomography **(e)** reveals smooth mass effect and mild rarefaction of posterior bony nasal septum and medial maxillary wall. Coronal computed tomography image **(f)** displaying focal cone-shaped hyperostosis with complete obstruction of the ostio-meatal unit shows smooth widening and no defects

with 3-cm defect, three cases with moderate disease, and two cases with mild disease. Only one case exhibited evidence of permeative lytic destruction in a pathologically proven squamous cell carcinoma (SCC) on top of IP. The bony changes are revealed as irregular permeative destruction at the lamina papyracea and the nasal septum. None of the non-SCC inverted papillomas exhibited this pattern of destruction.

Only a single case had intra-lesional *calcifications*. Six cases had focal *sclerosis*, two show linear smooth and plaque-like sclerosis of the osseous wall of the inferior turbinate (IT) in two nasal lesions. A third case showed focal sclerosis at the postero-lateral wall of the maxillary sinus in direct contact with the base

of the lesion. A fourth case had mild linear sclerosis along incomplete inter-sphenoid septum in a sphenoid sinus lesion, a fifth case had smooth minimal linear sclerosis at the base of the uncinate process close to a middle-meatus-epicentered lesion, nearly bisected by the uncinate process. A sixth case show frond-like-branching focal sclerosis at the base of a recurrent inverted papilloma, quite distinguishable from diffuse sclerosis of the operated sinus, mostly representing operative-induced osteogenesis.

Fifteen out of sixteen patients had involvement and extension through a drainage channel: Ten patients ($n = 10$) had extension through smoothly widened OMU unilaterally either in predominant nasal or maxillary sinus component; a case showed

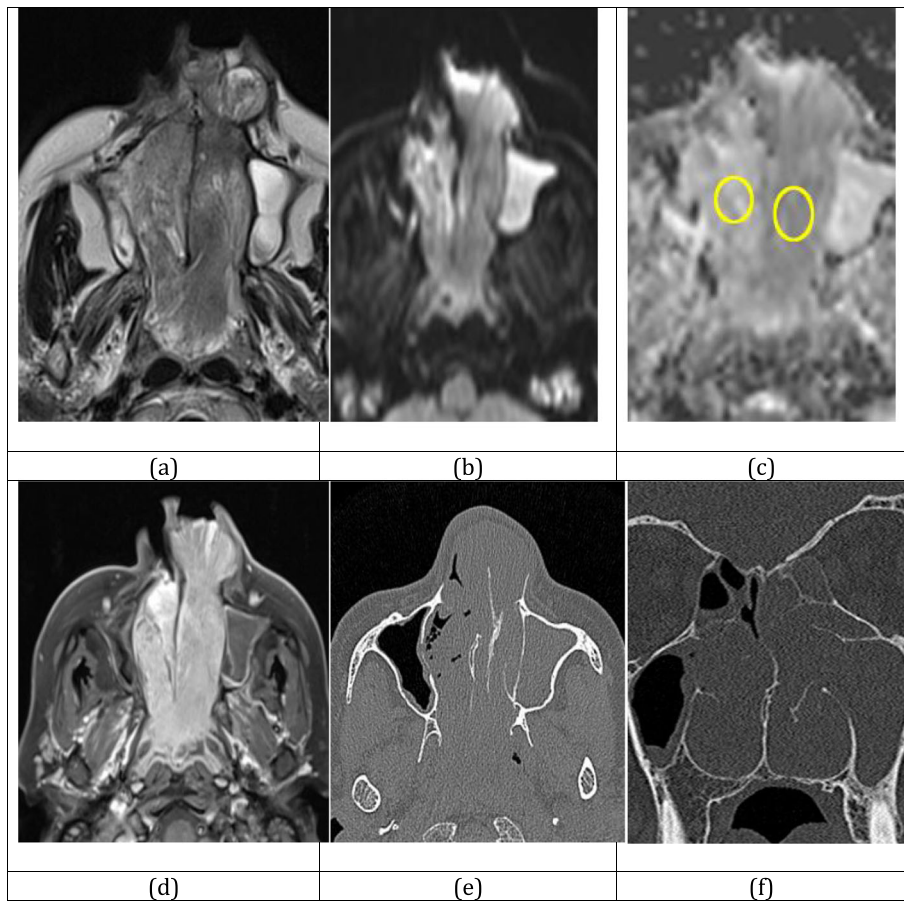


Fig. 3 A 65-year-old female with bilateral nasal obstruction and epistaxis. Axial T2-weighted image (a) reveals bilateral bi-nasal inverted papillomas, showing linear divergent and multi-directional scleroses. Axial diffusion and apparent diffusion co-efficient maps (a) and (b) reveal an apparent diffusion co-efficient of $1.5 \times 10^{-3} \text{ cm}^2/\text{s}$. Axial post-gadolinium-enhanced image (d) reveals striations less conspicuous than T2 images. Axial computed tomography image reveals smooth mass effect with linear scleroses at turbinate wall, where striations are divergent in relation to the site of focal hyperostosis. Coronal computed tomography image (f) shows the nasal lesions to have considerable intra-antral extensions through widened ostio-meatal units and through rarefied medial wall, as well as through widened post-meatal accessory ostia

bilateral OMU widening and obstruction; and four patients showed smoothly involved sphenoidal recess. Two patients had involvement of the frontal sinus, one is isolated, while the other is associated with OMU involvement.

Regarding magnetic resonance imaging findings (Table 3), visualization of T1-weighted images revealed diffusely T1 hyper-intense signal as compared to the masticatory muscles; four of the six cases exhibited slightly hyper-intense signal. The remaining ten cases revealed an iso-intense signal. All lesions revealed homogeneity of signal apart from a single case revealing iso-intense signal and focus of hyper-intense signal. Only three cases ($n = 3$) revealed a striated pattern, while all remaining ($n = 13$) showed non-specific pattern.

Regarding the T2 signal, five cases ($n = 5$) revealed diffusely iso-intense signal, two ($n = 2$) had hypo-intense signal, eight cases ($n = 8$) had diffusely hypo-to-iso-intense signal, while a single case revealed mixed areas of hypo and iso-intense signals. The *striated pattern* was seen in all cases ($n = 16$): Only two patients had convoluted pattern as visualized in the axial and coronal T1 + GAD and T2 STIR images. Four out of the 16 patients revealed a *cyst* within the confines of the mass, adequately differentiated from retained secretions. They revealed homogenous T2 signal of fluid with thin wall. Only a single cyst showed enhancement and three ($n = 3$) cysts did not enhance.

Regarding mass effect, extension and obstructive sinusitis, thirteen patients ($n = 13$) revealed *obstructive*

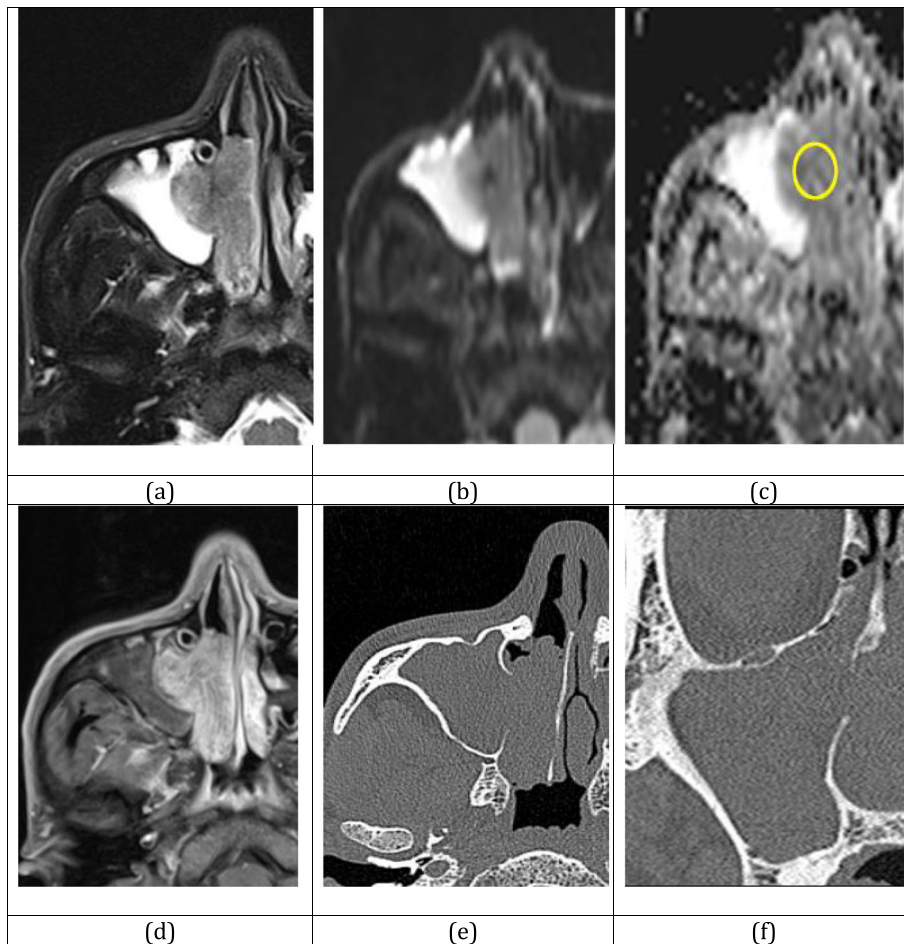


Fig. 4 A 52-year-old male presented with unilateral nasal obstruction and nasal inverted papilloma. Axial T2-weighted image reveals T2 linear divergent diffuse striations with T2 hypo-intensity with T2 'black-out' (b) reflected by compact cellularity and low apparent diffusion co-efficient value measuring $1.1 \times 10^{-3} \text{ cm}^2/\text{s}$ as seen in apparent diffusion co-efficient map (c). Axial post-gadolinium-enhanced image (d) reveals the striations to be more conspicuous than in T2 image. Axial computed tomography (e) reveals rarefied and widened post-meatal accessory ostium and smooth remodeling of medial maxillary sinus wall. Coronal computed tomography image shows sino-maxillary opacification continuous through smoothly widened ostio-meatal unit with smooth sclerosis of the middle turbinate wall

sinusitis and mass effect: Ten ($n = 10$) showed obstructive maxillary sinusitis, being mixed with ethmoidal sinusitis in two cases, and bilateral in one case. *Orbital extension* was seen in two cases, one of them had evidence of SCC with permeative pattern of destruction and lytic erosions at the lamina papyracea. Two patients had obstructive sphenoiditis in two sphenoidal-located lesion. Also, frontal sinus extension was noted in two cases, creeping through the fronto-ethmoidal recess.

Detailed evaluation of "striated pattern" revealed that all cases revealed the striated pattern ($n = 16$, Table 4); six patients ($n = 6$) showed divergent direction of the striations, four out of the six patients are divergent to the focal "sclerosis", and remaining two cases ($n = 2$) revealed "convoluted" pattern. Eight cases ($n = 8$) showed parallel direction, and two

patients revealed convoluted pattern of the striations. The subjective visibility of the "striated pattern" was made by two experienced senior and junior head and neck radiologists, with 23 and 12 years of head and neck radiology experience, respectively. This evaluation revealed: Higher T2 visibility in 11 cases, higher visibility at T1 + GAD-enhanced images in 3 cases, and equal visibility at both T2 and T1 + GAD in two cases.

Discussion

Inverted papilloma is a relatively uncommon neoplasm of the nasal cavity, constituting 0.5% to 4% of the whole primary nasal tumors and yet the commonest benign sino-nasal tumor [11]. The peak of incidence of IPs is in the fifth and sixth decades of life

Table 1 Demographics and clinical picture of all patients, with general morphology of the lesions by imaging

Patient no.	Age*	Sex**	Clinical symptomatology	Recurrent / primary	Laterality and side	Sino-nasal location	Size (cm)	Margins
(1)	39	M	Right nasal obstruction	Primary	Right	Nasal cavity and maxillary sinus	8.5	Lobulated
(2)	46	F	Nasal obstruction	Primary	Left	Nasal, between the middle and inferior turbinates	5.5	Elongated
(3)	67	F	Marked nasal obstruction	Primary	Bilateral	-Bi-nasal, more on left side, at middle and inferior turbinates -Left frontal sinus	10.5	Lobulated
(4)	69	M	Nasal obstruction	Primary	Right	Naso-ethmoido-frontal Crossing midline at nasal septum (SCC)	4.5	Lobulated
(5)	85	F	Nasal obstruction	Primary	Right.	Right maxillary sinus	5.5	Lobulated
(6)	43	M	Sinus headache	Primary	Right	Right maxillary sinus	2.5	Not applicable
(7)	65	M	Nasal obstruction	Primary	Midline	Spheno-nasal	7	Lobulated
(8)	76	F	Nasal obstruction	Primary	Left	Naso-ethmoidal +frontal extension	4.5	Elongated
(9)	75	F	Asymptomatic Incidental in CT brain	Primary	Right	Nasal -Between septum and turbinate and posterior recess	8.5	Elongated
(10)	54	M	Bilateral nasal obstruction	Primary	Bilateral	Naso-ethmoido-maxillary	10	Lobulated
(11)	53	M	Nasal obstruction	Primary	Right	Maxillo-nasal	5.4	Lobulated
(12)	37	M	Epistaxis	Primary	Right	Maxillary	4.5	Lobulated
(13)	43	M	Post-operative surveillance	Recurrent	Midline	Spheno-ethmoidal	1.7	Oval
(14)	40	M	Epistaxis	Primary	Left	Strictly nasal (middle meatus)	2.3	Elongated
(15)	29	F	Nasal obstruction-headache	Primary	Midline	Spheno-ethmoidal	4.5	Elongated
(16)	38	F	Routine surveillance	Recurrent	Left	Maxillary and ethmoidal	5.5	Lobulated

*Age represented in years

**Sex represented as Male = M, or Female = F

Table 2 Spectrum of bony changes of lesions including type of bony involvement and grading of changes

No.	Type of bony change	Bony walls involved	Extent of bony changes	Presence of focal hyperostosis	Calcification	Channel involvement
(1)	Remodeling and defects	Lateral wall and floor of maxillary sinus, right inferior turbinate	Severe 3 cm	None	None	Direct through medial wall and ostio-meatal unit
(2)	Remodeling only	Medial antral wall	Mild < 1 cm	None	None	Minimal extension through ostio-meatal unit
(3)	Remodeling and defects	Lateral nasal walls	Moderate 15 mm	The inferior turbinate	None	-Moderate extension through ostio-meatal unit with widening -Extension through frontal recess to FS
(4)	1-Remodeling and defects 2-Permeative destruction of septum	Right lamina papyracea remodeling defects. -Nasal septum destruction	Moderate 14 mm	None	Yes	Extension through ostio-meatal unit with widening
(5)	Remodeling only	Lateral nasal wall	Mild < 1 cm	The inferior turbinate	None	Moderate nasal extension through ostio-meatal unit with widening
(6)	None	None	None	None	None	Mild extension through Ostio meatal unit
(7)	Remodeling only	Sphenoid sinus roof and lateral walls	Mild < 1 cm	None	None	Widening of both sphenoid-ethmoidal recesses
(8)	None	None	None	None	None	-Minimal widening of frontal recess
(9)	Remodeling only	Nasal septum	Mild	None	None	Widening of sphenoid-ethmoidal recesses
(10)	Remodeling and defects	Lamina papyracea and bony nasal septum	Moderate 13 mm	None	None	Bilateral ostio-meatal units widening
(11)	None	None	None	None	None	Widening of ostio-meatal unit with no erosions
(12)	None	None	None	At postero-lateral wall of maxillary sinus	None	Widening of ostio-meatal unit with no erosions, No gross nasal extension
(13)	None	None	None	Along inter-sphenoid septum	None	Widening of ostio-meatal unit sphenoid-ethmoidal recesses
(14)	None	None	None	The uncinata process	None	Widening of ostio-meatal unit with no erosions
(15)	Remodeling and defects	Sphenoid sinus lateral walls and floor	Mild 4 mm	-	None	Widening of both sphenoid-ethmoidal recess
(16)	Remodeling and defects	Alveolar arch cortex	Mild 9 mm	Sclerosis Branching frond-like + post-operative neo-osteogenesis	None	None

Table 3 Detailed magnetic resonance imaging features of inverted papillomas in different MRI sequences

Patient no. *	T1 signal	T1 pattern	T2 signal	T2 pattern	Presence of cysts	Pattern on GAD enhancement	ADC value **	Mass effect and presence of obstructive sinusitis
(1)	Slightly hyper-intense	Striated	Hypo-to-iso	Striated	None	Striated	1.3	Mild ethmoidal-maxillary sinusitis
(2)	Iso-intense	None	Hypo	Striated	Yes -central	Striated enhancing cysts	1.6	Marked antro-choanal retention cyst
(3)	Iso-intense Tiny hyper-focus	None	Hypo-to-iso	Striated	Yes -peripheral	Striated	1.2	Mild antral ad frontal sinus extension and sinusitis
(4)	Iso-intense	None	Hypo-to-iso-intense	Striated	No cysts	Striated tiny internal cysts	1.5	Orbital extension- septal invasion and midline crossing
(5)	Iso-intense	Striated	Hypo-to-iso-intense	Striated	Yes - at periphery	Striated Non-enhanced cysts	1.4	Obstructive sinusitis
(6)	Hyper-intense	None	Hypo-to-iso-intense	Striated	No cysts	Striated	1.2	Minimal maxillary obstruction
(7)	Iso -intense	None	Hypo-to-iso-intense	Striated	Yes - small cysts	Striated Enhancing and non-enhancing cysts	1.1	Sphenoiditis
(8)	Iso-intense	None	Iso-intense	Striated	No cysts	Striated	1.1	Frontal sinus extension
(9)	Iso-intense	None	Hypo-to-iso-intense	Striated	No cysts	Striated	1.2	None (Limited within sinus cavity)
(10)	Slightly hyper-intense	None	Iso-intense	Striated (convoluted)	No cysts	Striated	1.2	Bilateral orbital extension Bilateral maxillary obstructive sinusitis
(11)	Slightly hyper-intense	None	Iso-intense	Striated linear	No cysts	Striated	1.0	Obstructive maxillary sinusitis
(12)	Slightly hyper-intense	Striated	Hypo-to-iso-intense	Striated linear	No cysts	Striated	1.2	Obstructive maxillary sinusitis
(13)	Iso-intense	None	Hypo-intense	Striated linear	No cysts	Striated	9.6	Obstructive sphenoiditis
(14)	Iso-intense	None	Iso-intense	Striated linear	No cysts	Striated	1.2	Obstructive maxillary sinusitis
(15)	Hyper-intense	None	Mixed iso and deeply hypo-intense	Striated linear	No cysts	Striated III defined	7.0	None (limited within sinus cavity)
(16)	Iso-intense	None	Iso-intense	Striated linear	No cysts	Striated	1.4	None (limited within sinus cavity)

ADC Apparent diffusion co-efficient (value represented as value $\times 10^{-3} \text{ cm}^2/\text{s}$)

Table 4 Magnetic resonance imaging features of the “striated pattern” sign, using different parameters

Patient no.	Diffuse versus non-diffuse	Direction of linear striations	Relation of striation to sclerosis	Visibility of striations in T2 versus post-gadolinium-enhanced image (GAD)
(1)	Diffuse	Parallel	-	T2 = GAD
(2)	Diffuse	Convolutd	-	T2 > GAD
(3)	Diffuse	Divergent	Divergent from sclerosis	T2 > GAD
(4)	Diffuse	Parallel	-	GAD > T2
(5)	Diffuse	Parallel	-	T2 > GAD
(6)	Diffuse	Parallel	-	T2 > GAD
(7)	Diffuse	Divergent	-	T2 > GAD
(8)	Diffuse	Parallel	-	T2 > GAD
(9)	Diffuse	Parallel	-	T2 > GAD
(10)	Diffuse	Convolutd	-	GAD > T2
(11)	Diffuse	Parallel	-	GAD > T2
(12)	Diffuse	Divergent	Divergent from sclerosis	GAD = T2
(13)	Diffuse	Divergent	Divergent from sclerosis	T2 > GAD
(14)	Diffuse	Divergent	Sclerosis bisects the lesion	T2 > GAD
(15)	Diffuse	Parallel	-	T2 > GAD
(16)	Diffuse	Divergent	Divergent from branching sclerosis	T2 > GAD

and still it has been reported in all age groups [12, 13]. Obviously, men are affected more often than women with a nearly 3-to-1 male-to-female predominance ratio [12, 13]. Our study revealed no sex preference and nearly equal proportions were reported, while age incidence was of old adults. IP most commonly arises from the lateral wall of the nose, with epicenter at the middle meatus. It can affect any sinus, the maxillary sinus being most common (Fig. 5), while isolated sphenoid sinus localization was reported as the lowest incidence (Figs. 6 and 7) [14–16]. *Bilateral* IP and multifocal involvement have been reported in the literature but still are an uncommon with uncommon finding of *intracranial*, skull base or orbital extension in IP without SCC [17, 18]. Our study revealed nasal involvement to have the highest prevalence.

CT is usually the initial investigation and shows red flag signs of sino-nasal mass. It is an excellent method for visualization of associated bony changes unlike a malignant tumor; IP causes bone remodeling (thinning and bowing) and resorption rather than osseous destruction [19]. Bone remodeling is reported to be most commonly at the medial wall of the maxillary sinus, followed by the lamina papyracea. The nasal septum is preserved until late in the disease course [20]. Our study revealed similar involvement of medial maxilla (= lateral nasal wall) and lamina papyracea. All patients had resorption pattern created by remodeling, and permeative erosion was seen in the single case with IP plus SCC (Table 5).

In IP, two patterns of *focal hyperostosis* have been described: the cone-shaped and the plaque-like hyperostosis; the former corresponds to tumor origin whereas the plaque-like hyperostosis may or may not be an indicator of tumor origin; identification of which has surgical importance, as its complete resection is required to avoid recurrence [21]. Six cases had focal hyperostosis: Only two had the cone-shaped appearance and both involved a maxillary sinus wall, one of them was post-operative recurrence. Plaque-like thin sclerosis was seen at the IT ($n = 2$), the uncinat process ($n = 1$) and intersphenoid septum ($n = 1$). The focal hyperostosis (cone-shaped) was suggested by several authors as a predictor of the IP implantation site, with a positive predictive value (PPV) of 89–95%, depending on reports. The underlying histopathology was suggested to be some form of chronic osteitis and hyper-vascularity, which may induce neo-osteogenesis or in other words, new bone formation. Still, our study did not correlate with post-operative specimens between sclerosis and origin of the tumor. Also, intra-lesional calcification is rare and non-specific; only one case presented with spotty calcified focus [21–25].

For MR imaging, multiple distinctive imaging features have been illustrated through literature. The lesion shows non-specific T1 iso-to-hyper-intense signal and T2 signal, nearly hypo-to-iso-intense to brain parenchyma or skeletal muscles with fat suppression

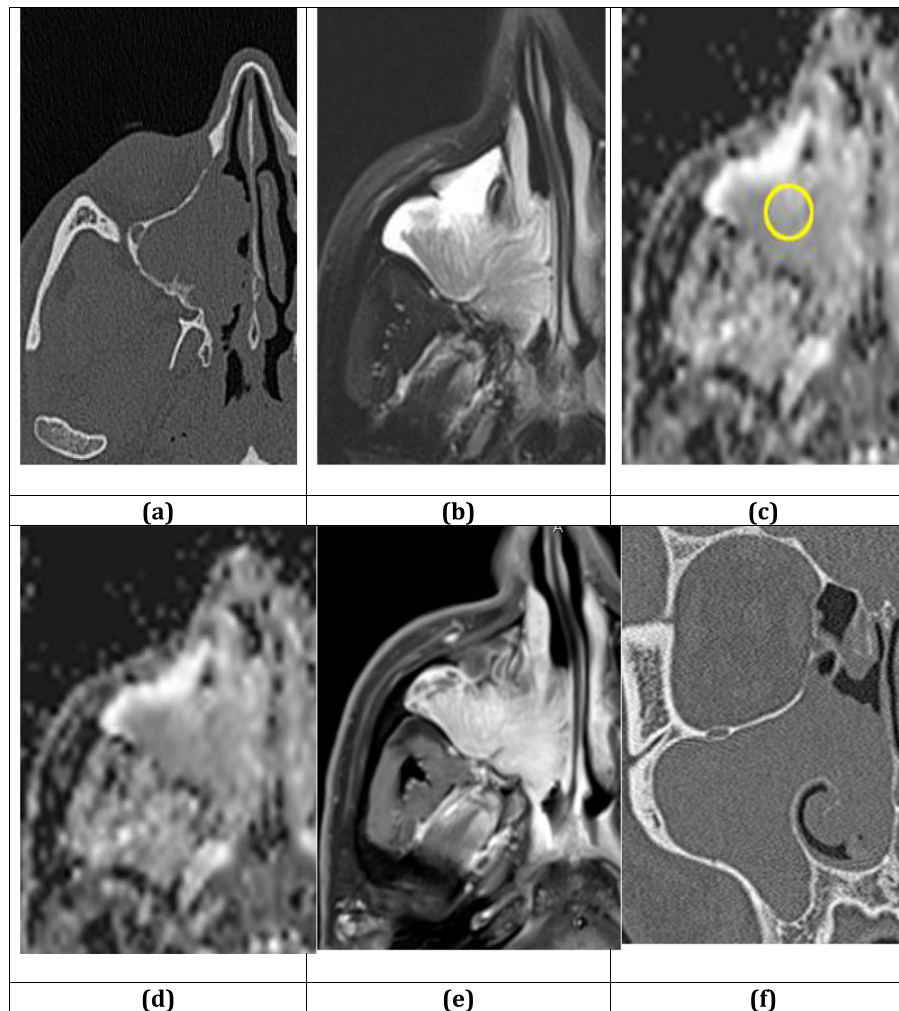


Fig. 5 A 37-year-old male with proven inverted papilloma of the right maxillary sinus. Axial computed tomography (a) reveals non-specific maxillary sinus opacification with focal hyperostosis at its postero-lateral wall. Axial T2-weighted image (b) shows linear striations divergent from the site of focal hyperostosis. T2 image also nicely differentiates obstructed secretions from solid mass reflecting moderate diffusivity with black-out effect of focal sclerosis at diffusion image (c) and apparent diffusion co-efficient value of $1.2 \times 10^{-3} \text{ cm}^2/\text{s}$, as measured in apparent diffusion co-efficient map (d). Axial fat suppressed post-gadolinium image (e) reveals linear striations may be less or equal to visibility in T2-weighted image. Coronal computed tomography image (f) shows smooth widening of the ostio-meatal unit with nasal extension of the maxillary mass

techniques. Following gadolinium, it shows evidence of contrast enhancement with adequate delineation of the tumors from the obstructive secretions with ruling out multiple pathologies as antro-choanal polyp, sinusitis, mucocele, and invasive fungal infections, as well as mapping the tumor extent. The diffusion pattern is non-specific and could not separate the IP from malignant lesions. Our study showed just similar general MRI features. Still this retrospective review selected the lesions with striated pattern on T2 and post-contrast T1 images [26–29]. Though Yousem et al. [30] stated that no signature pattern of MR imaging is specific of IP, later studies by Barnes et al.

[8] and Ojiri et al. [7] all showed a distinctive gross mucosal morphology of inverted papilloma called a convoluted cerebriform pattern. Different terms have been used as “convoluted”, “cerebriform”, “striated”, “gyriform”, and “columnar”; all are just synonyms for the same sign. We preferred the term “striated” in our study since it appears more general.

By histopathological examination, the IP is made of a compact cellular metaplastic epithelium and a sub-epithelial loose connective tissue. This pattern contributes to the striated pattern in the MRI: the compact epithelium contributes to linear hypo-intense signal and less enhanced line in enhanced images,

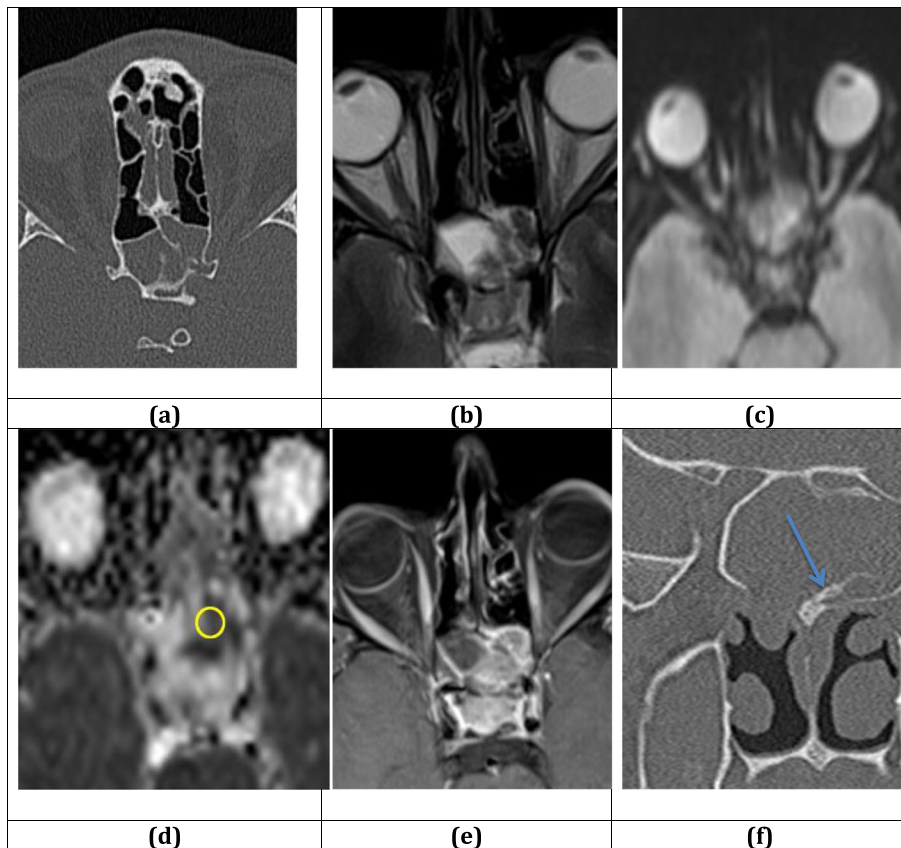


Fig. 6 A 35-year-old man with operated *sphenoid sinus* inverted papilloma. Axial post-operative computed tomography (a) reveals thick sclerotic septa that could be post-operative neo-osteogenesis rather than neoplastic induced. Axial T2-weighted reveals (b) the solid recurrent lesion as frond-like tissue on left side of the sphenoid cavity, with linear striations. Axial diffusion in (c) shows low spatial resolution reflected by too much bone-air interfaces, still apparent diffusion co-efficient map (d) nicely shows restricted tissue of only $0.9 \times 10^{-3} \text{ cm}^2/\text{s}$. Post-gadolinium image (e) shows enhanced solid component with too much less visibility of striations. Coronal computed tomography (f) reveals extension through the posterior nasal recess and endoscopic defect. Focal linear sclerosis of intra-sinus septum is seen (blue arrow) which may suggest surgery versus neoplasm induced

while the sub-epithelial loose connective tissue contributes to more T2 hyper-intense signal line and accumulation of gadolinium in variable concentrations according to its architecture. Barnes et al. [8] and Ojiri et al. [7] suggested that this convoluted pattern was specific in disagreement with the study by Yousem et al. [30] and suggested that a focal loss of this signature may suggest a focus of SCC. A study made by Maroldi et al. [9] made observation of this sign in 16 patients (69.5%) on T2-weighted images and 23 patients (100%) on contrast-enhanced T1-weighted images and was identified in only 1 (4.3%) of 23 other malignant sino-nasal tumors on both T2-weighted and contrast-enhanced T1-weighted images. They tried further to specify the sign by combining it with bony changes and concluded that this “striated columnar pattern” is a reliable MRI indicator of IP and reflects its histological architecture (positive predictive

value of 95.8%), and that the combination of this finding with the absence of extended bone erosion allows for the confident discrimination of IPs from malignant tumors with high diagnostic accuracy up to 97.8%. The study by Jeon et al. [10], a significant statistical difference in the prevalence of a CCP between IP (30 of 30, 100%) and other malignant sino-nasal tumors (17 of 128, 13%) with the overall sensitivity, specificity, positive predictive value, negative predictive value, and accuracy of CCP for the diagnosis of IP at 100%, 87%, 64%, 100%, and 89%, respectively.

In our study, we tried to emphasize this sign by showing details of the same sign: we meant to describe diffusivity of this lesion by a defining “diffuse” only when striated pattern covers > 90% of the longest tumoral diameter and this was seen in all striated lesions (100%). The study by Jeon et al. [10] stated that their study could have achieved more specificity

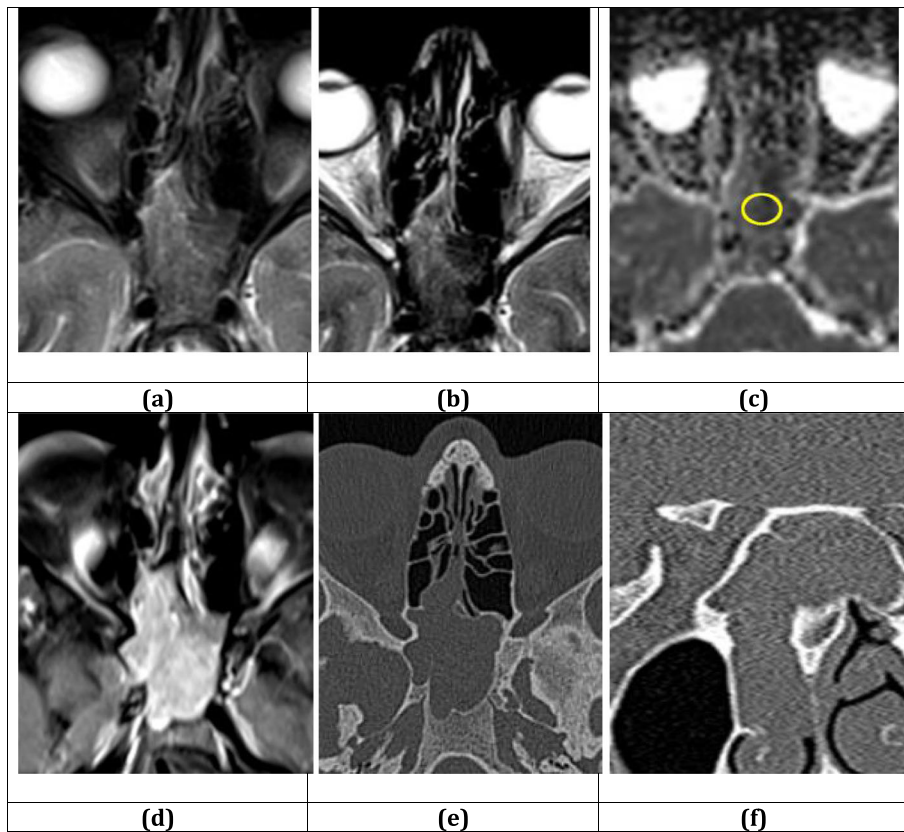


Fig. 7 A 37-year-old female with proven sphenoid sinus inverted papilloma. Axial T2-weighted (a) shows the solid tissue filling the sinus, with faintly depicted curved striations in multiple opposed direction, more resolved in axial non-FAT saturation T2-weighted image (b). Apparent diffusion co-efficient map (c) reflects the compact cellularity with a small apparent diffusion co-efficient value of $0.7 \times 10^{-3} \text{ cm}^2/\text{s}$. Axial post-gadolinium-enhanced image (d) reveals solid enhancing mass with very ill-defined striations. Axial computed tomography image (e) reveals non-specific opacity. Coronal computed tomography image (f) reveals lobulated sphenoid sinus opacity pedunculated through sphenoid-ethmoidal recess showing smooth widening

of this sign if they defined the term striated only when it is diffusely involving the lesion.

Further, the direction of the striated pattern was described in a certain pattern. Since the pathologic architecture follows a certain pattern of growth made by in-folding epithelium, a certain smooth direction of striations is expected. The 16 cases showed certain direction along most of the lesions like “linear”, “convoluted”, or “divergent”. This would not be expected in lesions with disorganized matrix. Furthermore, we considered that presence of intra-lesional cyst would not interrupt this sign. These cysts represent retention sub-epithelial cyst lined by glands and contains secretion. This would reveal smooth imperceptible line and T2 fluid signal, while enhancement could be only marginal or central and smooth, reflecting either retained secretions or lining epithelial glands, respectively. Relation of the striations to the focal hyperostosis was elucidated in the 6 patients with this finding: it showed divergent

growth in four ($n = 4$) and was bisected by the ostosis in one patient ($n = 1$), unrelated and away from the focal sclerosis in the six patients. The literature included reported cases of multiple bony attachments with higher post-operative recurrences. However, our retrospective survey revealed only single attachments [31].

Although prior imaging by Jeon et al. [10] showed that visibility of the sign was superior in post-GAD images, our study showed that T2 images are superior than enhanced images in 11 out of 16 cases; this may attributed to the fact that differential enhancement of the epithelium and sub-epithelial tissues is limited by the fact that an intrinsic variant exists; the sub-epithelial tissues are variable in cellularity and stroma which would lead to variable accumulation of contrast in these tissues that could be equal to the epithelium. An extrinsic variable is variability of timing acquisition and mode of dynamic contrast enhancement, which could limit the differential GAD enhancement.

Table 5 Distribution of the studied cases according to different parameters ($n = 16$)

	No. (%)
Degree of bony changes	
None	6 (37.5%)
Mild	6 (37.5%)
Moderate	3 (18.8%)
Severe	1 (6.3%)
Type of bony changes	
None	6 (37.5%)
Remodeling only	4 (25%)
Remodeling plus defects	6 (37.5%)
Presence of focal hyperostosis	
No	10 (62.5%)
Yes	6 (37.5%)
ADC value	
Mean \pm SD	2.1 \pm 2.5
Median (Min.–Max.)	1.2 (1 –9.6)
Pattern	
Diffuse	16 (100%)
Direction of growth	
Parallel	8 (50%)
Convoluted	2 (12.5%)
Divergent	6 (37.5%)
Relation of striation to sclerosis	
Divergent from sclerosis	3 (18.8%)
Sclerosis bisects the lesion	1 (6.3%)
Divergent from branching sclerosis	1 (6.3%)
Visibility of striations	
T2 > GAD	11 (68.8%)
T2 = GAD	2 (12.5%)
GAD > T2	3 (18.8%)

Obviously, our study has limitations. First, it is a retrospective study selectively retrieving the archived cases with the targeted imaging pattern. Secondly, a small number was examined (16 cases is still larger than sample size of 10 cases in the study made by Ojiri et al. [7]). This limited size rendered statistical analysis inappropriate. A third limitation is that our study did not include the pattern associated with metachronous SCC.

Conclusion

The inverted papillomas have potentially distinctive cross-sectional imaging; the most distinctive one is the “striated” pattern. This sign could be more specific when it is diffusely involving the lesion (> 90% of the longest diameter), related to or divergent from focal hyperostosis (if present), considered not interrupted by smooth

retention cyst, and showing better visibility in post-gadolinium contrast-enhanced images (as observed in our study). Also, presence of remodeling bony changes and smooth non-erosive resorptions are adding to the diagnostic yield of preoperative imaging study.

Abbreviations

ADC: Apparent diffusion co-efficient; CCP: Convoluted cerebriform pattern; CT: Computed tomography; FOV: Field of view; GAD: Gadolinium; IP: Inverted papilloma; IT: Inferior turbinate; MRI: Magnetic resonance imaging; MT: Middle turbinate; OMU: Ostio-meatal unit; SCC: Squamous cell carcinoma; TE: Time of ECHO; TR: Time of repetition

Acknowledgments

Not Applicable

Authors' contributions

ME provided the cases and final diagnoses, with detailed description of results. LE gave the idea, wrote the section of introduction and provided the whole references for introduction and discussion with making of figure legends. All authors read and approved the final manuscript.

Funding

This study had no funding from any resource.

Availability of data and materials

The datasets used and/or analyzed during the current study are available from the corresponding author on reasonable request.

Ethics approval and consent to participate

All procedures followed were in accordance with the ethical standards of the responsible committee on human experimentation (Institutional Review Board (IRB) of Alexandria General Hospital on 14th February 2017) and with the Helsinki Declaration of 1964 and later versions. Committee's reference number is unavailable (NOT applicable). No consent was obtained from the patients since it was a retrospective study.

Consent for publication

All patients included in this research gave written informed consent to publish the data contained within this study.

Competing interests

The authors declare that they have no competing interests.

Received: 26 September 2019 Accepted: 5 January 2020

Published online: 06 February 2020

References

- Wassef SH, Batra PS, Barnett S (2012) Review article: Skull base inverted papilloma: a comprehensive review. *International Scholarly Research Network*:1–34
- Sun Q, An L, Zheng J, Zhu D (2017) Advances in recurrence and malignant transformation of sinonasal inverted papillomas (Review). *Oncology Letters* 13:4585–4592
- Bayindir E, Mehmet F, Mahmut H, Kalcioğlu T, Zenginkinet T, Celik S (2019) Case Report. A case of inverted papilloma originating from the middle ear and review of the literature case reports in otolaryngology, pp 1–5
- Karkos PD, Khoo LC, Leong SC, Lewis-Jones H, Swift AC (2009) Computed tomography and/or magnetic resonance imaging for pre-operative planning for inverted nasal papilloma: review of evidence. *Journal of Laryngology and Otology* 123(7):705–709
- Loevner L, Sonnens A (2004) Imaging of neoplasms of the paranasal sinuses. *Neuroimaging Clinics of North America* 4:625–646
- Prado F, Weber R, Romano FR, Voegels RL (2010) Evaluation of inverted papilloma and squamous cell carcinoma by nasal contact endoscopy. *American Journal of Rhinology and Allergy* 24(3):210–214
- Ojiri H, Shimpe MU, Fukuda TK (2000) Potentially distinctive features of sinonasal inverted papilloma on MR imaging. *American Journal of Roentgenology* 175(2):465–468

8. Barnes L (2002) Schneiderian papillomas and nonsalivary glandular neoplasms of the head and neck. *Mod Pathol* 15:279–297
9. Maroldi R, Farina D, Palvarini L (2004) Magnetic resonance imaging findings of inverted papilloma: differential diagnosis with malignant sinonasal tumors. *Am J Rhinol* 18:305–310
10. Jeon TY, Kim HJ, Chung SK, Dhong HJ, Kim HY, Yim HJ, Kim ST, Jeon P (2007) Sinonasal Inverted Papilloma: Value of Convoluted Cerebriform Pattern on MR Imaging. *AJ Neuroradiol* 29:1556–1560
11. Garavello W, Gaini RM (2006) Incidence of inverted papilloma in recurrent nasal polyposis. *Laryngoscope* 116(2):221–223
12. Jurkiewicz D, Stryto A, Chomicki A, Koktysz R (2008) Endoscopic sinus surgery in a 102-year-old woman with inverted papilloma. *Otolaryngology* 138(4):537–539
13. Bhandary S, Singh RK, Shrestha S, Sinha AK, Badhu BP, Karki P (2006) Sinonasal inverted papilloma in eastern part of Nepal. *Kathmandu University Medical Journal* 4(16):431–435
14. Strek P, Zagolski O, Skladzien J, Oles K, Konior M, Hydzik-Sobocinska K (2007) Endoscopic surgical treatment of patients with isolated sphenoid sinus disease. *Otolaryngologia Polska* 61(3):254–259
15. Lee JT, Bhuta S, Lufkin R, Castro DJ (2003) Isolated inverting papilloma of the sphenoid sinus. *Laryngoscope* 113(1):41–44
16. Alba JR, Armengot M, Díaz A, Pérez A, Rausell N, Basterra J. Inverted papilloma of the sphenoid sinus, "Act-Oto-Rhino-Laryngologica Belgica 2002; 56(4): 399–4.
17. Salomone R, Matsuyama C, Filho G, De Alvarenga ML, Neto EM, Chaves AG (2008) Bilateral inverted papilloma. Case report and review of literature. *Rev Bras Otorrinolaringol* 74(2):293–296
18. Wright EJ, Chernichenko N, Ocal E, Moliterno J, Bulsara KR, Judson BL (2011) Benign inverted papilloma with intracranial extension: prognostic factors and outcomes. *Skull Base Rep* 1:145–150
19. Chawla A, Shenoy J, Chokkappan K, Chung R (2015) Imaging features of sinonasal inverted papilloma: a pictorial review. *Current Problems in Diagnostic radiology* 10:1–7
20. Anari S, Carrie S (2010) Sinonasal inverted papilloma: narrative review. *The Journal of Laryngology & Otology* 124:705–715
21. Lisan Q, Laccourreye O, Bonfils P (2016) Sinonasal inverted papilloma: from diagnosis to treatment. *European Annals of Otorhinolaryngology*:1–5
22. Lee DK, Chung SK, Dhong H-J, Kim HY, Kim H-J, Bok KH (2007) Focal hyperostosis on CT of sinonasal inverted papilloma as a predictor of tumor origin. *AJNR Am J Neuroradiol* 28:618–621
23. Bhalla RK, Wright ED (2009) Predicting the site of attachment of sinonasal inverted papilloma. *Rhinology* 47:345–348
24. Liang N, Huang Z, Liu H, Xian J, Huang Q, Zhou B (2017) Bone involvement: histopathological evidence for endoscopic management of sinonasal inverted papilloma. *Laryngoscope* 127:2703–2708
25. Head CH, Sercz JA, Luu Q, Collis J, Blackwell K (2007) Radiographic assessment of inverted papilloma. *Acta Oto-Laryngologica* 127:515–520
26. Ozturk K, Gawande R, Gencturk M, Boegel K, Caicedo-Granados E, Cayci Z (2018) Imaging features of sinonasal tumors on positron emission tomography and magnetic resonance imaging including diffusion weighted imaging: a pictorial review. *Clinical Imaging* 51:217–228
27. Kasbekar AV, Swords C, Attlmayr B, Kulkarni T, Swift AC (2018) Sinonasal papilloma: what influences the decision to request a magnetic resonance imaging scan? *The Journal of Laryngology & Otology* 132(7):584–590
28. Tatekawa H, Shimono T, Ohsawa M, Doishita S, Sakamoto S, Miki Y (2018) Imaging features of benign mass lesions in the nasal cavity and paranasal sinuses according to the 2017 WHO classification. *Japanese Journal of Radiology* 36(6):361–381
29. Sato E, Saiki T, Okochi Y (2018) A Study on 28 Cases with sinonasal inverted papilloma. *Practica oto-rhino- laryngologica* 152(5):40–41
30. Yousem DM, Fellows DW, Kennedy DW, Bolger WE, Kashima H, Zinreich SJ (1992) Inverted papilloma: evaluation with MR imaging. *Radiology* 185:501–505
31. Tong C, Patel N, Maina I, Triantafillou V, Yan C, Kuan E, Kohanski M, Pagiannopoulos P et al (2019) Inverted papilloma with multifocal attachment is associated with increased recurrence. *International Forum Allergy Rhinology* 9(8):865–869

Publisher's Note

Springer Nature remains neutral with regard to jurisdictional claims in published maps and institutional affiliations.

Submit your manuscript to a SpringerOpen[®] journal and benefit from:

- Convenient online submission
- Rigorous peer review
- Open access: articles freely available online
- High visibility within the field
- Retaining the copyright to your article

Submit your next manuscript at ► [springeropen.com](https://www.springeropen.com)
